Proceedings of the
Annual Stability Conference
Structural Stability Research Council
Louisville, Kentucky, April 13-16, 2021

Computation of flexural buckling loads via curvature-based displacement interpolation

Michael H. Scott[1], Mark D. Denavit[2]

Abstract
The calculation of critical loads for flexural buckling of columns remains a relevant topic of practical and theoretical interest. In addition to well-known solutions for prismatic columns, closed-form expressions are available for the critical loads of non-prismatic columns; however, the expressions are often complex, as are finite element analyses that require a refined mesh in order to achieve accurate solutions. Eigenvalue analysis of the curvature-based displacement interpolation (CBDI) influence matrix, which is a by-product of the force-based frame element formulation of geometric nonlinearity, is an alternative approach to the calculation of the critical loads. This approach is simple and efficient and can be applied to non-prismatic columns and other cases where the flexural stiffness varies along the length of the member. The accuracy of the critical loads depends on the underlying quadrature rule from which the influence matrix is formed. Comparisons with previously published results show this eigenvalue approach gives accurate first mode critical loads when using at least four Gauss integration points. The development of this approach provides a novel perspective on a classical problem and highlights the rich information regarding the critical loads contained within the CBDI influence matrix.

1. Introduction

Column buckling has been the focus of extensive mathematical research, dating back to the mid-18th century with the work of Euler, who provided a direct solution to the governing differential equation for bending of a prismatic column. While stability criteria in modern design codes remain rooted in Euler's buckling formula, non-prismatic columns are often employed for reasons of economy, efficiency, and aesthetics. In addition, the flexural stiffness of an initially prismatic member can vary due to partial yielding of the cross section, corrosion, fire, and other hazards. Whether varying flexural stiffness is intentional or unanticipated, buckling loads for such column members must be computed for reliable structural design and assessment. With only a handful of closed-form solutions available, most solutions for the buckling loads of columns with varying flexural stiffness rely on numerical solutions or finite element analysis.

[1] Professor, Oregon State University, <michael.scott@oregonstate.edu>
[2] Assistant Professor, University of Tennessee, Knoxville, <mdenavit@utk.edu>

Analytic solutions for the buckling loads of non-prismatic columns were derived by Timoshenko and Gere (1961) using Bessel functions. Dalal (1969) developed analytic solutions for buckling of stepped and other non-conventional columns. Numerical solutions were obtained by Smith (1988) and Eisenberger (1991) using energy methods and power series, respectively. More recently, Darbandi et al (2010) used a singular perturbation method to obtain closed-form solutions for the buckling loads of tapered columns.

The objective of this paper is to show that a by-product of a formulation for geometrically nonlinear force-based frame elements provides a general approach to computing buckling loads for non-prismatic columns. Numerical examples show the accuracy of the proposed method for critical buckling loads of prismatic, stepped, and tapered columns using Gauss integration to define the CBDI influence matrix.

2. Governing Equations

Although the calculation of buckling loads by the CBDI procedure does not require finite element analysis, the procedure is a by-product of a geometrically nonlinear force-based frame finite element formulation. This section summarizes the pieces of the finite element analysis formulation that are relevant to calculating buckling loads using CBDI.

In two dimensions, force-based elements are formulated with three degrees of freedom (DOFs) in a basic system, free of rigid body displacement modes. As shown in Fig. 1, the first DOF corresponds to axial force at end *J* of the element while the second and third DOFs correspond to bending moment at ends *I* and *J*, respectively.

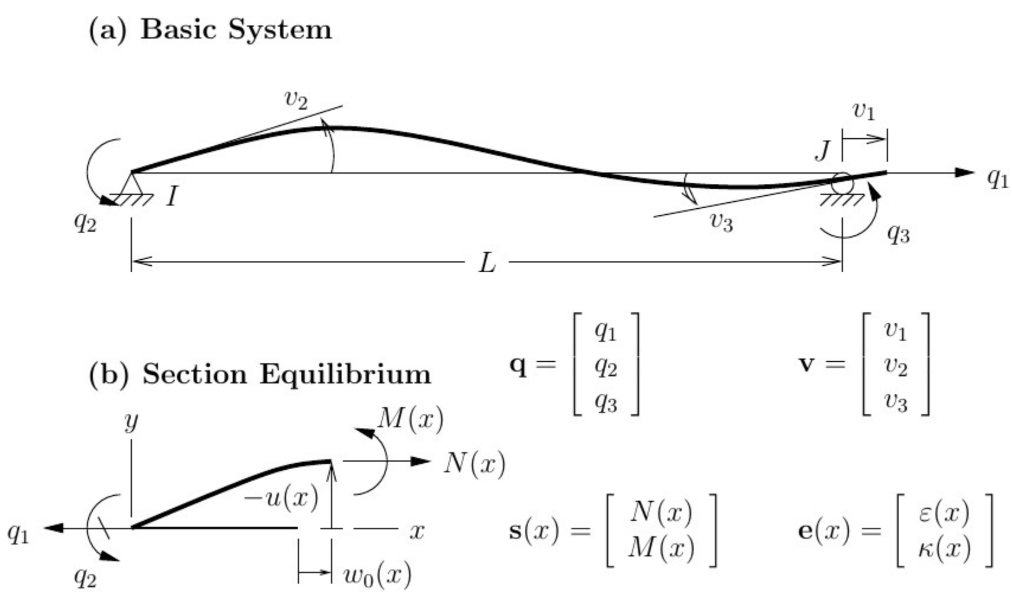

Figure 1: Basic system and section equilibrium for force-based frame elements in two dimensions.

Although it is straightforward to extend the CBDI formulation to account for shear deformation and member loads, the focus of this work is on the common case of Bernoulli beam theory with no member loads.

2.1 Equilibrium

The homogeneous solution to beam equilibrium is expressed in matrix-vector form

$$\mathbf{s}(x) = \mathbf{b}(x, u(x))\mathbf{q} \tag{1}$$

where **q** is the vector of basic forces and **s** is the vector of section forces at any location along the beam. In addition to the geometrically linear solution of a linear distribution of bending moment, the force interpolation matrix, **b**, includes the effect of axial load on internal bending moment

$$\mathbf{b}(x, u(x)) = \begin{bmatrix} 1 & 0 & 0 \\ -u(\xi) & \xi - 1 & \xi \end{bmatrix} \qquad \xi = x/L \tag{2}$$

The amplification of internal bending moment by the axial load is commonly known as the P-δ effect. The locations where the beam equilibrium relationship in Eq. (1) is evaluated depends on the element integration method.

2.2 Constitution

At each integration point, the section forces in **s** are related to their conjugate deformations, collected in a vector **e**, by the section flexibility matrix, $\mathbf{f}_s$,

$$\mathbf{f}_s \equiv \frac{\partial \mathbf{e}}{\partial \mathbf{s}} = \begin{bmatrix} \frac{\partial \varepsilon}{\partial N} & \frac{\partial \varepsilon}{\partial M} \\ \frac{\partial \kappa}{\partial N} & \frac{\partial \kappa}{\partial M} \end{bmatrix} \tag{3}$$

which is typically defined in terms of elastic constants, E, A, and I. As shown in the forthcoming buckling examples, it is not necessary for the section flexibility to be constant along the element, i.e., the CBDI formulation handles non-prismatic members.

2.3 Calculation of Transverse Displacement

In the CBDI formulation, the curvature along an element is approximated with Lagrange interpolating functions

$$\kappa(\xi) = \sum_{j=1}^{N_p} l_j(\xi)\kappa_j \qquad \xi = x/L \tag{4}$$

where κ_j is the curvature at the j^{th} integration point and l_j is the j^{th} Lagrange polynomial

$$l_j(\xi) = \frac{\prod_{i=1, i \neq j}^{N_p} (\xi - \xi_i)}{\prod_{i=1, i \neq j}^{N_p} (\xi_j - \xi_i)} \tag{5}$$

Note that the j^{th} Lagrange polynomial evaluates to 1 at the j^{th} integration point and 0 at all other integration points, i.e., $l_i(x_j)=\delta_{ij}$.

As described in Neuenhofer and Filippou (1998), after double integration of the curvature field in Eq. (4), application of the boundary conditions of the basic system, and expansion of the Lagrangian polynomials in a monomial basis, the transverse displacement field in the basic system can be expressed as a matrix-vector product

$$\mathbf{u} = -L^2 \mathbf{l}^* \boldsymbol{\kappa} \tag{6}$$

where $\boldsymbol{\kappa}$ is a vector of curvatures at all integration points and $\mathbf{l^*}$ is the CBDI influence matrix

$$\mathbf{l}^* = \mathbf{h}\mathbf{g}^{-1} \tag{7}$$

where **h** is a matrix of integrated Lagrange polynomials that satisfy the boundary conditions of the basic system

$$\mathbf{h} = \begin{bmatrix} (\xi_1^2 - \xi_1)/2 & (\xi_1^3 - \xi_1)/6 & \dots & (\xi_1^{N_p+1} - \xi_1)/(N_p(N_p+1)) \\ (\xi_2^2 - \xi_2)/2 & (\xi_2^3 - \xi_2)/6 & \dots & (\xi_2^{N_p+1} - \xi_2)/(N_p(N_p+1)) \\ \vdots & \vdots & \ddots & \vdots \\ (\xi_{N_p}^2 - \xi_{N_p})/2 & (\xi_{N_p}^3 - \xi_{N_p})/6 & \dots & (\xi_{N_p}^{N_p+1} - \xi_{N_p})/(N_p(N_p+1)) \end{bmatrix} \tag{8}$$

and **g** is a Vandermonde matrix of simple monomials

$$\mathbf{g} = \begin{bmatrix} 1 & \xi_1 & \xi_1^2 & \dots & \xi_1^{N_p-1} \\ 1 & \xi_2 & \xi_2^2 & \dots & \xi_2^{N_p-1} \\ \vdots & \vdots & \vdots & \ddots & \vdots \\ 1 & \xi_{N_p} & \xi_{N_p}^2 & \dots & \xi_{N_p}^{N_p-1} \end{bmatrix} \tag{9}$$

Both **h** and **g** are square matrices with dimension $N_p \times N_p$.

2.4 Derivative of Transverse Displacement

The eigenvalue analysis shown in the following section depends on the derivative of the transverse displacements at the integration points with respect to the basic forces. To find this derivative, Eq. (6) is differentiated with respect to **q** along with the chain rule

$$\frac{\partial \mathbf{u}}{\partial \mathbf{q}} = -L^2 \mathbf{l}^* \frac{\partial \boldsymbol{\kappa}}{\partial \mathbf{q}} = -L^2 \mathbf{l}^* \sum_{j=1}^{N_p} \frac{\partial \kappa_j}{\partial \mathbf{s}_j} \frac{\partial \mathbf{s}_j}{\partial \mathbf{q}} \tag{10}$$

Differentiating the equilibrium relationship in Eq. (1) with respect to basic forces then applying the chain rule gives

$$\frac{\partial \mathbf{s}}{\partial \mathbf{q}} = \mathbf{b} + \frac{\partial \mathbf{b}}{\partial u} \mathbf{q} \frac{\partial u}{\partial \mathbf{q}} \tag{11}$$

The derivative of the section equilibrium matrix, **b**, with respect to transverse displacement is

$$\frac{\partial \mathbf{b}}{\partial u} = \begin{bmatrix} 0 & 0 & 0 \\ -1 & 0 & 0 \end{bmatrix} \tag{12}$$

Substituting Eqs. (11) and (12) into Eq. (10) gives the following expression

$$\frac{\partial \mathbf{u}}{\partial \mathbf{q}} = -L^2 \mathbf{l}^* \mathbf{F}_{\kappa s} \mathbf{B} + q_1 L^2 \mathbf{l}^* \mathbf{F}_{\kappa M} \frac{\partial \mathbf{u}}{\partial \mathbf{q}} \tag{13}$$

where **B** is a $2N_p \times 3$ matrix of section force interpolation matrices

$$\mathbf{B} = \begin{bmatrix} \mathbf{b}_1 \\ \mathbf{b}_2 \\ \vdots \\ \mathbf{b}_{N_p} \end{bmatrix} \tag{14}$$

and $\mathbf{F}_{\kappa s}$ and $\mathbf{F}_{\kappa M}$ are N_p × $2N_p$ and N_p × N_p blocked matrices, respectively, of section flexibility coefficients corresponding to the derivative of curvature with respect to selected section forces

$$\mathbf{F}_{\kappa s} = \begin{bmatrix} \frac{\partial \kappa_1}{\partial N_1} & \frac{\partial \kappa_1}{\partial M_1} & 0 & 0 & \dots & 0 & 0 \\ 0 & 0 & \frac{\partial \kappa_2}{\partial N_2} & \frac{\partial \kappa_2}{\partial M_2} & \dots & 0 & 0 \\ \vdots & & \vdots & & \ddots & & \vdots \\ 0 & 0 & 0 & 0 & \dots & \frac{\partial \kappa_{N_p}}{\partial N_{N_p}} & \frac{\partial \kappa_{N_p}}{\partial M_{N_p}} \end{bmatrix} \quad \mathbf{F}_{\kappa M} = \begin{bmatrix} \frac{\partial \kappa_1}{\partial M_1} & 0 & \dots & 0 \\ 0 & \frac{\partial \kappa_2}{\partial M_2} & \dots & 0 \\ \vdots & \vdots & \ddots & \vdots \\ 0 & 0 & \dots & \frac{\partial \kappa_{N_p}}{\partial M_{N_p}} \end{bmatrix} \tag{15}$$

Then, solving Eq. (13) for the derivative of transverse displacements gives

$$\left(\mathbf{I} - q_1 L^2 \mathbf{l}^* \mathbf{F}_{\kappa M}\right) \frac{\partial \mathbf{u}}{\partial \mathbf{q}} = -L^2 \mathbf{l}^* \mathbf{F}_{\kappa s} \mathbf{B} \tag{16}$$

3. Eigenvalue Analysis

At critical buckling loads, where the transverse displacements increase unboundedly with respect to basic forces, the determinant of the matrix on the left-hand side of Eq. (16) will be zero

$$\det\left(\mathbf{I} - q_1 L^2 \mathbf{l}^* \mathbf{F}_{\kappa M}\right) = 0 \tag{17}$$

The roots, q_1, of the characteristic polynomial that arises from the determinant give the critical buckling loads. An alternative interpretation of critical buckling is that multiplication of the matrix by a non-zero vector **x** gives the zero vector

$$\left(\mathbf{I} - q_1 L^2 \mathbf{l}^* \mathbf{F}_{\kappa M}\right) \mathbf{x} = \mathbf{0} \tag{18}$$

This expression leads to the standard eigenvalue equation

$$\left(-L^2 \mathbf{l}^* \mathbf{F}_{\kappa M}\right) \mathbf{x} = \left(\frac{1}{q_1}\right) \mathbf{x} \tag{19}$$

where the sign on q_1 has been flipped so that it is positive in compression, contrary to the standard definition shown in Fig. 1. As a result, the eigenvalues of $(-L^2 \mathbf{l}^* \mathbf{F}_{\kappa M})$ correspond to the reciprocal of the critical buckling loads q_1 and the eigenvectors, $\mathbf{x}$, are the associated buckled shapes, i.e., the transverse displacement at each of the N_p integration points. Given that the size of the matrix $(-L^2\mathbf{l}^*\mathbf{F}_{\kappa M})$ is dictated by the number of integration points, at most N_p eigenpairs $(1/q_1, \mathbf{x})$ can be computed according to Eq. (19).

With the weighting factors supplied by the section flexibility matrix, $\mathbf{F}_{\kappa M}$, it is straightforward to account for non-prismatic members and weakened sections in computing buckling loads via eigen-analysis of Eq. (19). The accuracy of the buckling modes computed from Eq. (19) depends on the numerical properties of the underlying element integration rule, as shown in the following examples.

4. Examples

Applications to buckling problems show the utility of the CBDI buckling approach. First, the CBDI approach is applied to the common case of a prismatic column, then the non-prismatic cases of stepped and tapered columns. All examples assume pin-pin boundary conditions.

4.1 Prismatic columns

For a prismatic, linear-elastic column, $\mathbf{F}_{\kappa M}$ reduces to a diagonal matrix where each entry is $1/EI$. As a result, the eigenvalue solution in Eq. (19) should lead to the well-known Euler buckling load

$$P = \frac{\pi^2 EI}{L^2} \tag{20}$$

The important factor is the number of integration points and their locations, which affect the size and numerical quality, respectively, of the CBDI influence matrix, **l***.

The stability variable $\psi^2 = PL^2/EI$ computed from the lowest eigenvalue, $q_1 = P$, of Eq. (19) for an increasing number of Gauss integration points is shown in Fig. 2. With three or more Gauss points, the computed solution matches the expected result. Although integration point locations based on other quadrature methods is possible, Gauss integration is chosen for its high accuracy.

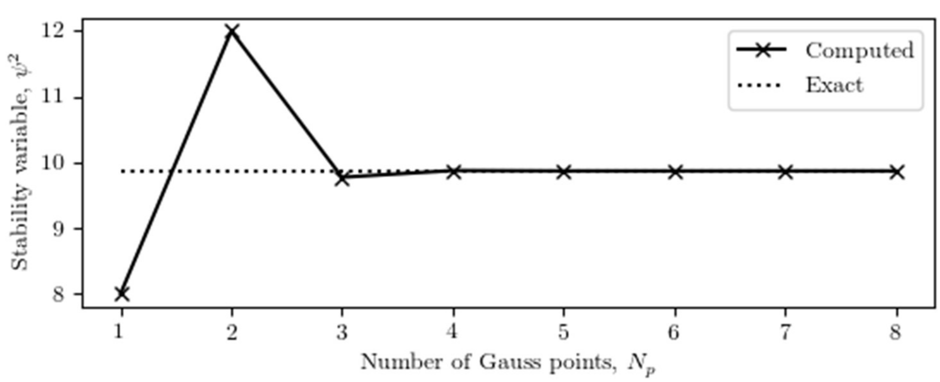

Figure 2: Critical buckling load (stability variable) for a prismatic, pin-pin column computed by CBDI procedure for an increasing number of Gauss integration points.

4.2 Stepped columns

Dalal (1969) developed closed-form solutions for buckling of non-conventional columns, including stepped columns and columns with distributed and intermediate axial loads. The case of an unsymmetrically stepped column is shown in Fig. 3 where α and β parametrize the step.

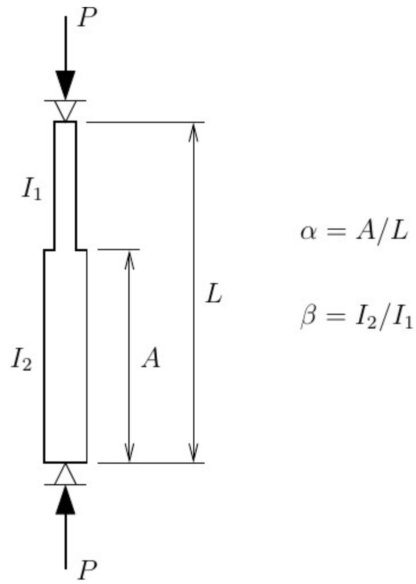

Figure 3: Parameters for unsymmetric stepped column (adapted from Dalal (1969)).

The CBDI approach is applied to the stepped column by mapping the integration point locations across the step, i.e., over the element domain L, then assigning the appropriate section flexibility, either $1/EI_1$ or $1/EI_2$ based on the integration point location relative to the step.

The critical buckling loads computed by the CBDI approach are shown in Fig. 4 for three values of β over the full range of α. The CBDI calculations lead to a piecewise constant variation of buckling load as the step location, defined by α, crosses integration point locations. As more integration points are used, the variation of buckling load converges to the exact solution. However, the CBDI influence matrix becomes ill-conditioned when the number of integration points becomes large due to the terms in the last column of **h** and **g** (Eqs. 8 and 9) being raised to the N_p+1 and N_p–1 powers, respectively.

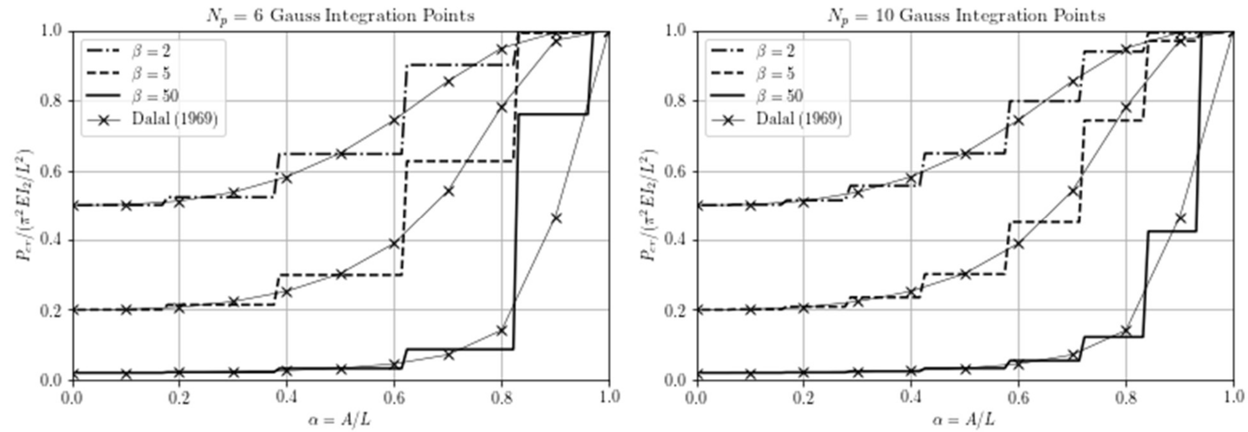

Figure 4: Critical buckling load for stepped column computed by CBDI approach for 6 and 10 Gauss integration points.

4.3 Tapered columns

The buckling solution for columns with smooth tapers is difficult to derive analytically (Timoshenko and Gere 1961). Instead, various numerical solutions for the critical buckling loads of tapered columns have been developed (Smith 1988, Eisenberger 1991, Darbandi et al 2010). A common test case shown in Fig. 5 is of a column with linear variation of in-plane width. Assuming a rectangular section with constant out-of-plane width, this variation gives rise to a cubic variation in the second moment of cross-sectional area. The change in flexural stiffness due to taper of the in-plane width is parametrized by η. Note that η=1 gives the prismatic case shown in the first example.

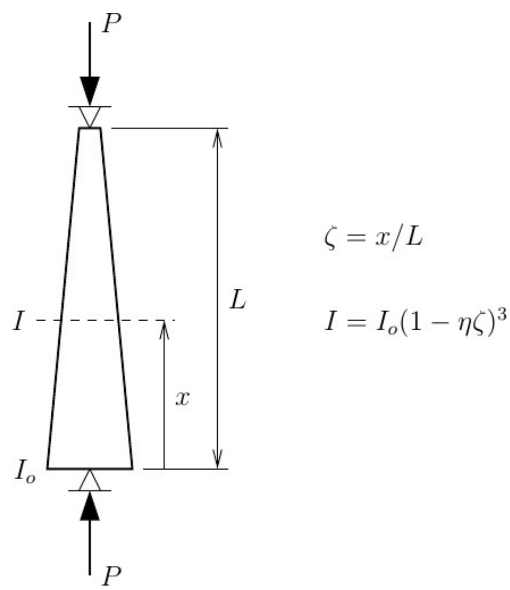

Figure 5: Parameters for tapered column (adapted from Darbandi et al (2010)).

Applying the CBDI approach to the critical buckling loads of the tapered column in Fig. 5 gives the results shown in Fig. 6. Four cases are shown for η ranging from 0.2 to 0.8. In all cases, compared to the FEM results presented in Darbandi et al (2010), the CBDI approach gives accurate results for three or more Gauss integration points.

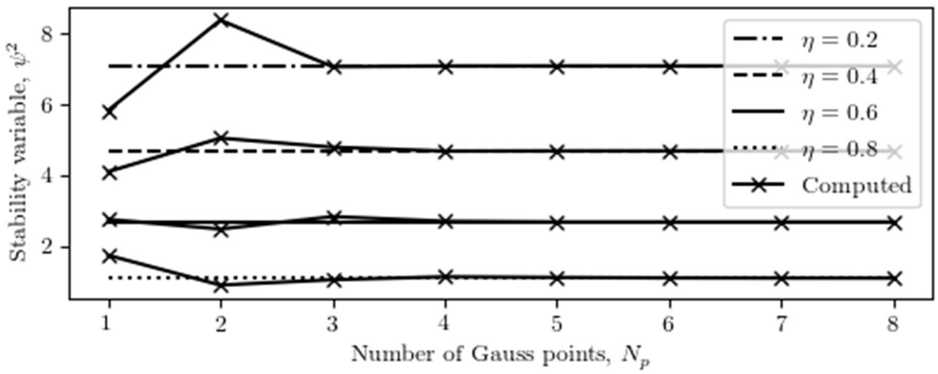

Figure 6: Critical buckling load for column computed by CBDI approach for range of tapers.

Although the foregoing examples focused on Bernoulli beams, the approach can be extended to buckling of shear deformable beams through the CSBDI approach (Jafari et al 2010). In addition, when forming the CBDI influence matrix, other quadrature methods, e.g., Gauss-Lobatto, Newton-Cotes, and Chebyshev, can be applied; however, these methods generally give lower accuracy than Gauss quadrature and thus require more integration points. Finally, it is straightforward to extend the CBDI approach to other non-conventional cases of column buckling (Dalal 1969) such as distributed and intermediate axial loads.

5. Conclusions

The curvature-based displacement interpolation (CBDI) influence matrix contains rich information regarding the critical buckling loads of column members. As a stand-alone approach, independent of the finite element formulation in which it is typically employed, eigenvalue analysis of the CBDI influence matrix is a convenient tool for computing buckling loads of non-prismatic columns.

Examples with prismatic, stepped, and tapered columns demonstrated the accuracy of the approach. For prismatic and smooth tapered columns, four Gauss points was sufficient to obtain accurate critical buckling loads. The CBDI buckling equations are easily programmed in Python or MATLAB where the eigenvalue solution of a 4×4 matrix is trivial. Stepped columns have a discontinuity in flexural stiffness that can only be resolved by using more integration points. Higher mode buckling loads also require more integration points, and thus a larger CBDI influence matrix.

References

Dalal, S.T. (1969). "Some non-conventional cases of column design." *AISC Engineering Journal*, 6 (1) 28-39.

Darbandi, S., Firouz-Abadi, R. Haddadpour, H. (2010). "Buckling of variables section column under axial loading." *ASCE Journal of Engineering Mechanics*, 136 (4) 472-476.

Eisenberger, M. (1991). "Buckling loads for variable cross-section members with variable axial forces." *International Journal of Solids and Structures*, 27 (2) 135-143.

Jafari, V., Vahdani, S.H., Rahimian, M. (2010). "Derivation of the consistent flexibility matrix for geometrically nonlinear Timoshenko frame finite element." *Finite Elements in Analysis and Design*, 46 (12) 1077-1085.

Neuenhofer, A., Filippou, F.C. (1998). "Geometrically nonlinear flexibility-based frame finite element." *ASCE Journal of Structural Engineering*, 124 (6) 704-711.

Smith, W. G. (1988). "Analytic solutions for tapered column buckling." *Computers and Structures*, 28 (5) 677-681.

Timoshenko, S. P., and Gere, J. M. (1961). Theory of elastic stability, 2nd ed., McGraw-Hill, New York.